Raman Spectroscopic Study on Acetic Acid Clusters in Aqueous Solutions: Dominance of Acid−Acid Association Producing Microphases

Nobuyuki Nishi,*,†,‡ Takakazu Nakabayashi,† and Kentaroh Kosugi†,‡

Institute for Molecular Science, Myodaiji, Okazaki 444-8585, Japan, and Graduate School for Advanced Studies, Myodaiji, Okazaki 444-8585, Japan

Received: August 18, 1999; In Final Form: October 12, 1999

With the addition of water into liquid acetic acid, the C═O stretching vibration band of acetic acid shows a high-frequency shift from 1665 to 1715 cm^{-1}. This means that the hydrogen bond of the C═O group of acetic acid is not as strong as those seen in liquid acetic acid or in CCl_4 solution (in which the band appears at 1668 cm^{-1}). A bent type hydrogen bond is accountable for this observation. On the other hand, the increase of acetic acid in water drastically decreases the intensity of the hydrogen-bonded O−H stretching Raman band of water at 3200 cm^{-1}. This suggests that acetic acid breaks the hydrogen-bond networks of water. Low-frequency $R(\bar{\nu})$ spectra of acetic acid/water binary solutions are re-examined with new experimental data and ab initio molecular orbital analysis of intermolecular vibrational modes. The $R(\bar{\nu})$ spectrum of the aqueous mixture at $x_A = 0.5$ bears a very close resemblance to that of the acetic acid/methanol mixture with $x_A = 0.5$, indicating that the molecular complexes responsible for the Raman spectra are acetic acid clusters. The calculated low-frequency Raman feature of a side-on type dimer with bent-type hydrogen bonds based on ab initio molecular orbital theory reproduces the observed Raman pattern nicely. Any evidence of the formation of stable acid−water pairs is not found in the low-frequency Raman spectra. Furthermore, an isosbestic point is seen in the region of $0.1 \leq x_A$ (mole fraction of acetic acid) ≤ 0.5, and another one is also observed in $0.5 \leq x_A \leq 1.0$. The observed spectra in the region of $0 < x_A < 0.5$ are reproduced simply by linear combinations of the pure water spectrum and the spectrum at $x_A = 0.5$. These results strongly suggest the presence of the two microphases with homogeneously associated molecules: a water cluster phase and an acetic acid cluster phase. The spectral change in $0.5 < x_A < 1.0$ is attributed to the coexistence of the acetic acid cluster phase in aqueous environment and the acid associated phase characteristic of liquid acetic acid.

1. Introduction

In our recent letter articles,[1,2] we reported the presence of isosbestic points in the $R(\bar{\nu})$ spectra of ethanol/water[1] and acetic acid/water mixtures;[2] the former system showed a single isosbestic point over the whole mixing ratios, and the latter system exhibited two isosbestic points different in the mixture compositions: the water-rich region, $0 \leq x_A$ (mole fraction of acetic acid) ≤ 0.5 and the acid-rich region, $0.5 \leq x_A \leq 1.0$. In the case of ethanol/water mixtures, the observed spectra were reproduced with linear combinations of the pure water spectrum and the pure ethanol spectrum. This indicates that the mixtures are composed of microphases of water associates and ethanol associates and there is little contribution to the spectra from ethanol/water complexes. Kaatze and co-workers obtained a similar conclusion on the basis of dielectric spectroscopy of carboxylic acid/water mixtures.[3] They found the presence of two relaxation terms and attributed it to the existence of two microphases, one with high and the other one with low water content. The water-rich phase was assumed to fill the space between the acid-rich microphase aggregates. They also reported that in monohydric alcohol/water mixtures the fluctuation correlation lengths do not exceed some molecular diameters[4] in contrast to much longer lengths expected for acid-rich phases in carboxylic acid/water mixtures. This is in good agreement with our previous study by mass spectrometric analyses of clusters isolated from liquid droplets.[5−7] The study with this method for carboxylic acid/water mixtures demonstrates that the acid−acid association becomes more stable for a longer alkyl chain that causes hydrophobic interaction in aqueous media.[8]

Low-frequency Raman spectroscopy provides information on local structure of solutions coupled with hindered translational and librational motions. Waldstein and Blatz reported the low-frequency Raman spectra of liquid acetic acid and its solution in water.[9] However, we could not observe any spectrum similar to those they reported.[2] They also stated that predominant associated species in the aqueous mixture is probably an open dimer of acetic acid. The Rayleigh wing spectra have been presented with $R(\bar{\nu})$, the intrinsic Raman scattering activity.[1,10−14] The Raman signals originating from dipole-induced dipole interaction are dominated by the interaction between the neighboring molecules.[1,10] In fact, Madden and Impey succeeded in reproducing the observed $R(\bar{\nu})$ spectrum of water from molecular dynamics (MD) simulation using the MCY potential with 125 molecules.[10] They found that the 185 cm^{-1} component is prominently correlated with the bimolecular in-plane mode of hydrogen bonded water molecules. The vibrational frequencies and Raman intensities of such bimolecular modes can be estimated by the ab initio molecular orbital method with a reliable basis set. In this report, we demonstrate the usefulness

* To whom correspondence should be addressed. E-mail: Nishi@ims.ac.jp.
† Institute for Molecular Science.
‡ Graduate University for Advanced Studies.

10.1021/jp9929061 CCC: $18.00
Published on Web 11/25/1999

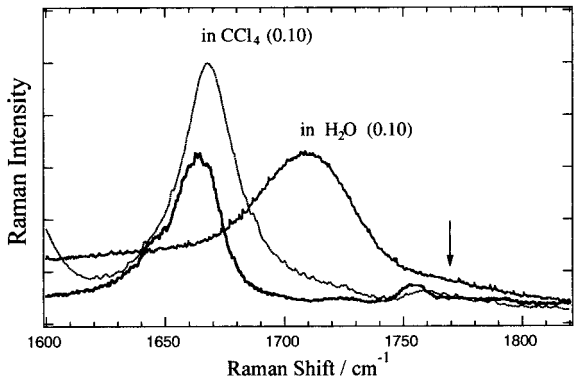

Figure 1. Raman spectral shifts of the C═O stretching vibration band of acetic acid in a crystalline sample at 286 K (thick solid line), in water (thin solid line), and in CCl_4 (dotted line). The mole fraction of acetic acid is 0.1 in both the solutions, and the temperature of the solutions is 297 K. A vertical arrow at 1770 cm^{-1} indicates the position where high-temperature liquid acetic acid at 343 K shows a high-temperature band attributed to the free (or nonbonded) C═O.

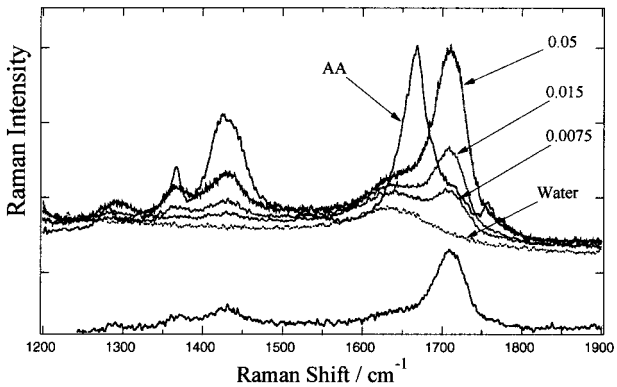

Figure 2. Raman spectra of acetic acid aqueous solutions with x_A = 0.0075, 0.015, and 0.05 in the region of 1200−1900 cm^{-1}. The spectra of water and crystalline acetic acid at 286 K (AA) are also shown for comparison. The intensity of AA is reduced to approximately 1/15. The bottom spectrum is obtained by subtracting the water spectrum from the spectrum of the aqueous solution at $x_A = 0.015$.

of the theoretical calculation of intermolecular vibrational modes for the assignment of low-frequency Raman spectra of binary solutions.

2. Experimental Section

High purity water was prepared by a Puric-Z water purifier (Organo Co. Ltd.). Acetic acid of spectroscopy grade (more than 99.7 v/v %; Wako Pure Chemical Industries) was used without further purification. Acetic acid aqueous solutions were sealed in 6 mm Pyrex glass tubes after degassing of carbon dioxide by repeating the freezing and evacuation. Raman spectra were measured in the low-frequency region (14−400 cm^{-1}) at 293 K with a NR-1800 Raman spectrophotometer (JASCO) equipped with a triple monochromator and a cooled photomultiplier tube (Hamamatsu Photonics R943-02). Scattered light was measured at an angle of 90° relative to the exciting laser beam. The 514.527 nm (19 435 cm^{-1}) line from an argon ion laser (NEC) was used with a power of 150 mW at the sample. The GAUSSIAN 94 program package[15] was used on a DEC AlphaStation 500.

3. Results and Discussion

Spectral Shifts of Raman-Active Intramolecular Vibrations. Frequency shifts of intramolecular vibrations provide qualitative information on the structural change related to solute−solvent and solute−solute interactions. In particular, hydrogen-bond formation of the C═O group of a carboxylic acid causes a clear spectral shift to a lower wavenumber dependent on the degree of its binding strength.[16,17] Bertie and Michaelian studied the Raman spectrum of the gas-phase cyclic dimer.[18] They observed a C═O stretching vibration band of the cyclic dimer at 1681.5 cm^{-1} and a monomer band at 1789.6 cm^{-1}. Ng and Shurvell applied the factor analysis method to the Raman spectra of acetic acids in aqueous solution.[16] They assigned the major components in the spectrum of the mixture with $x_A = 0.17$ to monomer and cyclic dimer bands with the band positions at 1696 and 1673 cm^{-1}, respectively, although they are overlapped forming a broad band. The difference is only 23 cm^{-1} in contrast to the large difference of 108 cm^{-1} in the gas phase. The spectrum of the aqueous mixture with x_A = 0.10 is shown in Figure 1 with a thin solid line. In the figure, the spectrum of an acetic acid/carbon tetrachloride mixture with $x_A = 0.10$ and that of crystalline acetic acid at 286 K are also shown with a dotted line and a thick solid line, respectively, for comparison. As clearly seen, the peak of the broad band is located at 1710 cm^{-1} shifted by 50 cm^{-1} to the higher wavenumber from the crystalline band position and 42 cm^{-1} from the peak of the carbon tetrachloride mixture band. At 343 K, the spectrum of the acetic acid and carbon tetrachloride mixture with $x_A = 0.10$ shows intensity increment of the bands at 1760 cm^{-1} and the strong low-wavenumber bands at 1668 cm^{-1} show eminent intensity decrease. The band at 1760 cm^{-1} is assigned to acetic acid monomer species and that at 1668 cm^{-1} to the C═O group linearly hydrogen-bonded with the OH group of another acid. The temperature increase may induce the dissociation of the linear hydrogen bond. The dissociation energies are estimated to be 10 (±2) kcal/mol from the temperature dependence. Crystalline acetic acid has a network structure composed of strong linear hydrogen bonds.[19,20] In carbon tetrachloride, acetic acid molecules are expected to form a cyclic dimer structure or an aggregate structure similar to crystalline acetic acids. The spectral shift from the C═O stretching band of the free species amounts to approximately 100 cm^{-1}. This is in good coincidence with the shift in the gas phase.[18] The peak position of the C═O stretching band of the aqueous solution is located just between the wavenumber for the free C═O and that of the strongly hydrogen bonded one. As the factor analysis by Ng and Shurvell showed, the broad band at 1710 cm^{-1} is analyzed as a composite of two components.[18] Both of them cannot be attributed to the C═O group either with a linear hydrogen bond or free from any hydrogen bond. A bent-type hydrogen bond can explain this shift to the intermediate position. Figure 2 shows the concentration dependence of the C═O stretching band in a low acid concentration region. The spectra obtained after the subtraction of the water spectrum (mostly ν_2 vibration) show essentially no concentration dependence of the spectral shape in the region of $0.2 \geq x_A \geq 0.0075$. The subtracted spectrum of the mixture at $x_A = 0.015$ is shown in the lower part of Figure 2, where one can see an asymmetric band shape of the C═O stretching band at 1710 cm^{-1}. This is attributed due to the presence of overlapping two bands at 1695 and 1715 cm^{-1}.

The O−H stretching vibrations of acetic acid and water are expected to exhibit large spectral shifts on hydrogen bond formation. Figure 3 shows the Raman spectra of aqueous solutions with $x_A = 0.1$ and 0.2 in the region from 2700 to 3700 cm^{-1}. The spectra of liquid acetic acid and water are also displayed for comparison. The strongest band at 2945 cm^{-1} is the C−H stretching band of acetic acid. The water spectrum

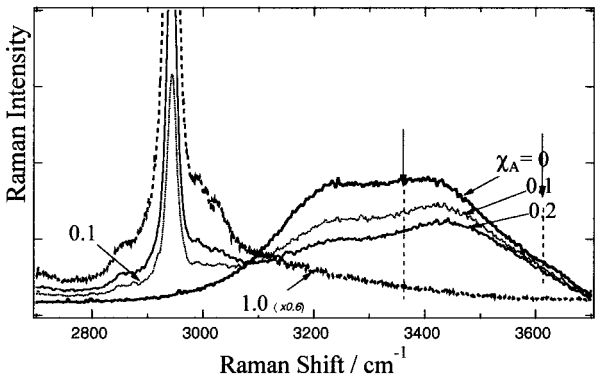

Figure 3. Raman spectra of acetic acid aqueous solutions with x_A = 0.10 and 0.20 in the region of 2700−3700 cm^{-1}. The spectra of liquid acetic acid and water are also shown for comparison.

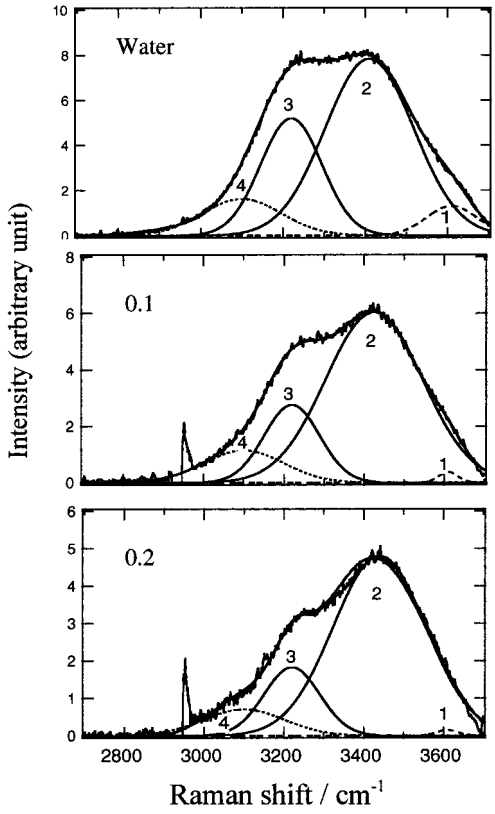

Figure 4. Relative intensity change of the Gaussian components in the water spectra. The water spectra of the aqueous solution of acetic acid were obtained by subtracting the scaled spectrum of liquid acetic acid from the original spectra shown in Figure 3. The scaling factor was obtained so as to extinguish the sharp C−H band of acetic acid at 2940 cm^{-1}. The assignment of components 1−4 is given in the text.

shows the two peaks at 3230 cm^{-1} and 3420 cm^{-1}. The band contour of the water spectrum is reproduced by assuming 4 Gaussian components with the band centers at 3610, 3410, 3220, and 3100 cm^{-1}. The result of the Gaussian analysis of the water spectrum is shown at the top of Figure 4, where the four components are designated as components 1, 2, 3, and 4, respectively. On the basis of the degree of wavenumber shift, component 1 at 3610 cm^{-1} is assigned to the ν_1 mode of a water molecule of which two hydrogen atoms are both free from hydrogen bonding and corresponds to the 3657.1 cm^{-1} band in the gas phase.[21] Component 2 at 3410 cm^{-1} is assigned to the ν_1 mode of a weakly associated water molecule of which one hydrogen is bonded to a neighbor water but the other one is not bonded. In principle, this kind of water molecule should

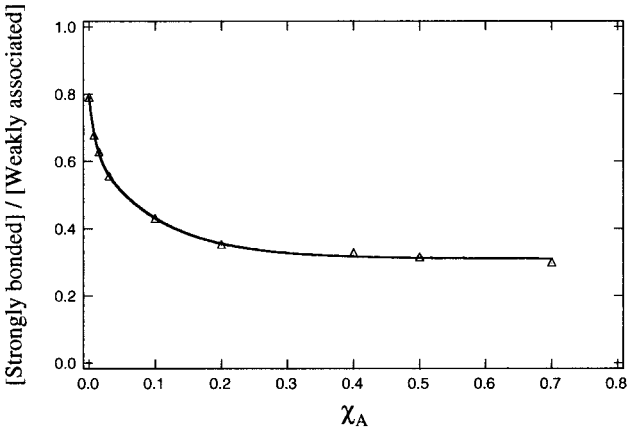

Figure 5. Intensity ratio of the strongly bonded O−H components to the weakly associated components as a function of x_A (acetic acid mole fraction). The solid curve is a double-exponential function expressed by eq 1.

show two O−H stretching bands. The very broad feature of this band could be attributed to the overlapping two components of the weakly associated water molecule. Another possibility is due to a water dimer with nonlinear hydrogen bonds such as bifurcated species. It is very difficult to assign this broad component to any specific structure of weakly associated dimers. Component 3 at 3220 cm^{-1} is assigned to the ν_1 mode of a water of which two hydrogen atoms are bonded to neighbor molecules. This strongly bonded water must be in a different situation than that of the icy water with tetrahedral coordination that appears as component 4 at 3100 cm^{-1} in Figure 4. Hare and Sorensen[22] observed a strong Raman band of ice at 3100 cm^{-1}. Here, we call the molecules responsible for component 2 as weakly associated water molecules and the molecules responsible for the two hydrogen atoms bonded (responsible to components 3 and 4) as strongly bonded water molecules.

The lower two spectra are obtained by subtracting the scaled liquid acetic acid spectrum from the spectra of the acetic acid/water mixtures with x_A = 0.1 (middle) and 0.2 (bottom). The subtraction is performed in order to eliminate the C−H stretching band of acetic acid. However, because of a little spectral shift of this band, the subtraction provides a negative and a positive spike with equivalent intensity. With increasing acid concentration, the decrease in the strongly bonded components becomes much eminent, suggesting the breaking of the water structure. The ratios of the strongly bonded components to the weakly associated component at various molar fractions of acetic acid are plotted and fit to a double-exponential function in Figure 5:

$$\text{[strongly bonded]/[weakly associated]} = 0.252 + 0.114\exp(-1.186x_A) + 0.220\exp(-13.5x_A) \quad (1)$$

At a concentration of x_A = 0.05, the second component becomes equivalent to the third component that is the main term in the high x_A region. This concentration of x_A = 0.05 appears to have an important meaning in a later section.

Low-Frequency Raman Spectra. The Rayleigh wing spectra have been presented in a function of the so-called $R(\bar{\nu})$,[10−14,23]

$$R(\bar{\nu}) = I(\bar{\nu})(\bar{\nu}_0 - \bar{\nu})^{-4}\bar{\nu}[1 - \exp(-hc\bar{\nu}/kT)] \quad (2)$$

where $\bar{\nu}_0$ is the frequency of the exciting laser line (in cm^{-1}) and $I(\bar{\nu})$ is scattered light intensity of frequency $\bar{\nu}$. The $R(\bar{\nu})$ spectrum has the practical advantage of essentially removing

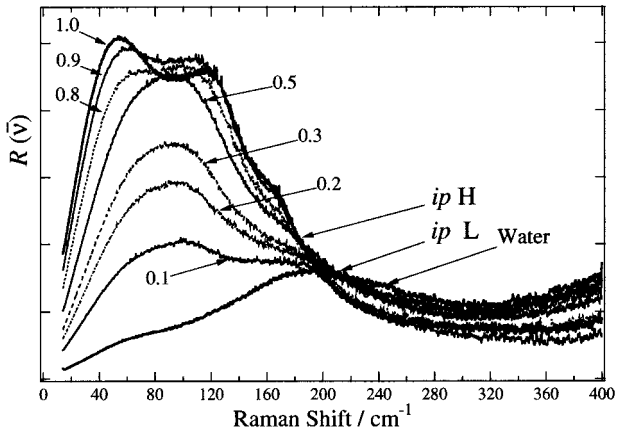

Figure 6. $R(\bar{\nu})$ spectra of acetic acid/water mixtures at $x_A = 0$ (water), 0.1, 0.2, 0.3, 0.5, 0.8, 0.9, and 1.0 (liquid acetic acid). *ip*H and *ip*L stand for the isosbestic points in the high acetic acid region of $0.5 \leq x_A \leq 1.0$ and in the low acid region of $0.1 \leq x_A \leq 0.5$, respectively.

the intensity of the exciting laser line and extracting from the measured Raman spectrum a quantity that is related to the vibrational density of states. Figure 6 shows the $R(\bar{\nu})$ spectra of acetic acid/water mixtures at $x_A = 0$ (water), 0.1, 0.2, 0.3, 0.5, 0.8, 0.9, and 1.0 (liquid acetic acid). With increasing acetic acid from $x_A = 0.1$ to 0.5, an evolving spectral component is seen in the region from 50 to 120 cm^{-1}. This component has the same spectral feature as the spectrum at $x_A = 0.5$. From $x_A = 0.5$ to 1.0, the change is very much different from that in the low concentration region; the intensity change is not so large but the structural change is drastic. The spectrum at $x_A = 0.5$ is completely different from that of liquid acetic acid ($x_A = 1.0$). The presence of the isosbestic points at 210 cm^{-1} in the low-concentration region and 180 cm^{-1} in the high-concentration region may suggest the three states of associates: pure water cluster state; 1:1 mixture state; pure acetic acid state. Thus, we have attributed the 1:1 mixture state to the acetic acid−water cluster state in ref 2. However, we face a difficult situation for this assignment with new experimental and theoretical results.

In Figure 7a, the low-frequency Raman spectra of the acetic acid/water mixtures at $x_A = 0.5$ (thick line) and 0.3 (thin line) are compared with that of acetic acid/methanol mixture at $x_A = 0.3$ (thin broken line). The intensity scale is normalized for the peak intensities of the respective spectra. Although the spectra at $x_A = 0.3$ contain some contribution from either the water clusters or the methanol clusters seen in the respective pure liquids, the main feature of the spectral pattern is similar. The same molecular cluster(s) must be responsible to the low-frequency spectra of the acetic acid/water and the acid/methanol mixtures. Vibrational wavenumbers of molecular complexes of acetic acid with methanol are expected to show a large difference from those of acetic acid−water complexes because of the mass difference between the partners. Thus, the two heterodimers are expected to show spectral features different from each other. In fact, the ab initio calculation (Figure 7d) of acetic acid−water and acetic acid−methanol dimers at the HF/6-31++G** level provides Raman-active vibrations at higher wavenumbers in the region of 150−400 cm^{-1}. The geometries of the optimized dimers are shown in parts c and d of Figure 8, respectively. We also examined the Raman activity spectra of various acetic acid homodimers.[24] The side-on type acetic acid dimer shown in Figure 8a provides a Raman structure in Figure 7b that well reproduces the spectral feature of the three spectra in Figure 7a. The cyclic dimer with the structure shown in Figure 8b also provides the four bands in the region of 50−160 cm^{-1}. The

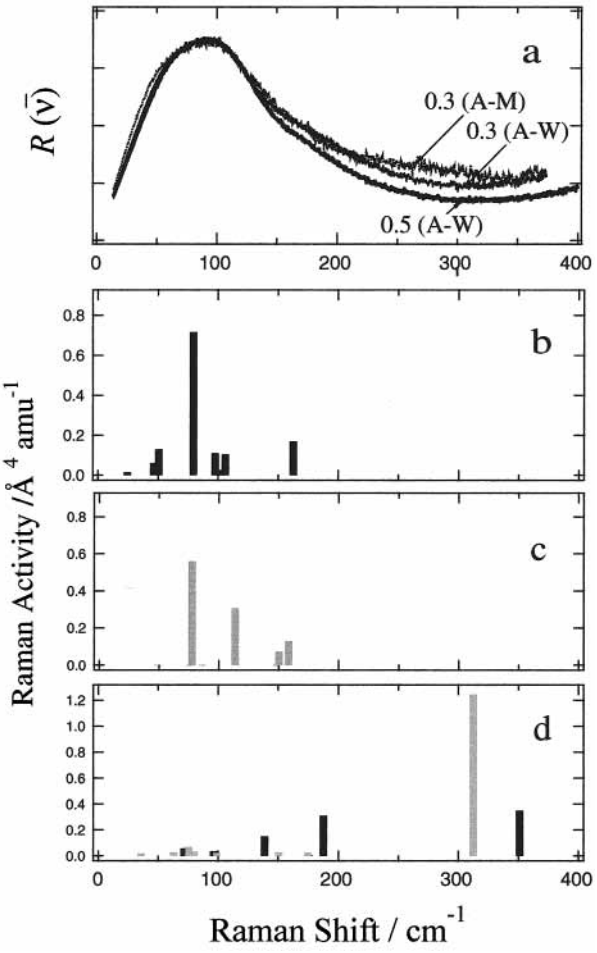

Figure 7. (a) Low-frequency Raman spectra of the acetic acid/water mixtures at $x_A = 0.5$ (thick line), at $x_A = 0.3$ (thin line), and the spectrum of acetic acid−methanol mixture at $x_A = 0.3$ (thin broken line). The intensity scale is normalized for the peak intensities of the respective spectra. (b) HF/6-31++G** level calculation of Raman activities of bimolecular vibrations of a side-on dimer the structure of which is shown in Figure 8a. (c) The same level calculation of a cyclic dimer shown in Figure 8b. (d) Calculated Raman activities of acetic acid−water (black bars) and acetic acid−methanol (gray bars) heterodimers structures of which are shown in parts c and d of Figure 8, respectively.

integrated Raman intensity of the intermolecular bands of the side-on dimer is stronger than that of the cyclic dimer. The calculated spectral pattern of the side-on dimer shows a better fitting to the observed spectrum rather than that of the cyclic dimer. However, it is not as conclusive for the assignment of the observed low-frequency spectra because of the broad feature of the observed spectra. From the calculated spectra, one can only say that the main origin of the low-frequency spectra must be acetic acid dimer units. As shown in a previous section, however, the spectral position of the intramolecular C═O stretching vibration indicates that the C═O group is not as strongly hydrogen bonded. Any dimer structure with a linear hydrogen bond is not able to explain this point but the side-on dimer with the bent-type hydrogen bonds accounts for all of the observed results. A problem is how the side-on dimer unit can be well stabilized in aqueous environment despite its small binding energy in the gas phase compared with that of the cyclic dimer.

The calculated binding energies for the acid−water dimer, the acid−methanol dimer, the side-on type homodimer, and the cyclic homodimer are −6.46, −6.34, −5.27, and −12.31 kcal/

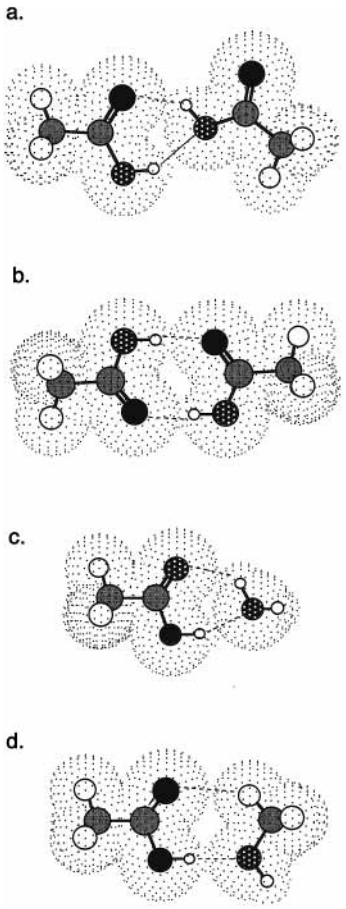

Figure 8. Structures of acetic acid dimers (a), a cyclic dimer (b), an acetic acid−water heterodimer (c), and an acetic acid−methanol dimer (d) obtained by ab initio calculations at the HF/6-31++G** level. The binding energies of the respective dimers are given in the text.

TABLE 1: Dipole Moments of Acetic Acid Homo- and Heterodimers Calculated at the HF/6-31++G Level**

	dipole moment/debye
side-on dimer	4.011
cyclic dimer	0.000
AA-water	1.106
AA-MeOH	2.220

mol, respectively, at the HF/6-31++G** level. These values are corrected for the zero-point vibrational energies. So, the gas-phase dimerization energy of the side-on type dimer is not favorable to the heterodimers, although the differences from the values of the two heterodimers are approximately 1 kcal/mol. Apparently the binding energy of the cyclic dimer is more than twice as large as that of the side-on type dimer in the gas phase. Thus, in the gas phase we have little possibility of observing the side-on dimer. Aqueous solution is a polar environment where polar solute species are well stabilized by the surroundings.

Table 1 shows the calculated dipole moments of the above four acetic acid homo- and heterodimers. The side-on type dimer exhibits the largest dipole moment (4.011 D) among them, in contrast to the null dipole moment of the cyclic dimer. In the concentration region studied here, dipole−dipole interaction between the dimer pairs can also be important for generating higher clusters. The energy of dimer−dimer interaction between the cyclic dimers is on the order of van der Waals interaction energies, while that between the antiparallel pairs of two side-on dimers is expected to be sufficiently large. Recently, we have performed a calculation of the binding energy change in aqueous

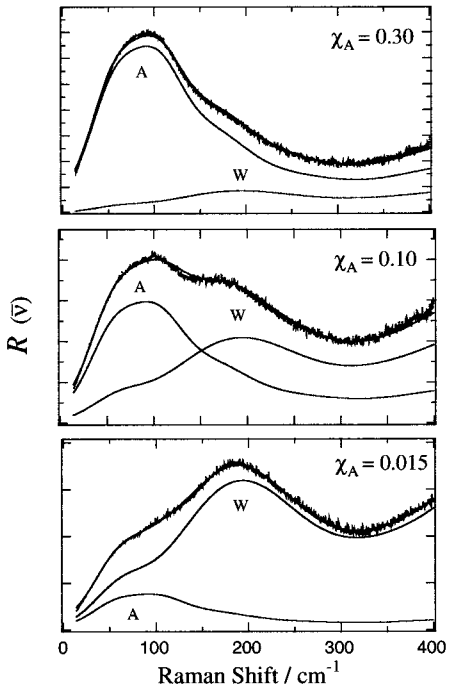

Figure 9. Decomposition of the observed $R(\bar{\nu})$ spectra of the binary solutions with $x_A = 0.015$, 0.10, and 0.30 into linear combinations of the R($\bar{\nu}$) spectra of pure water and the mixture with $x_A = 0.5$. The sum spectra calculated by a least-squares fitting method are shown with solid lines.

environment of the two dimers by the RISM-SCF method, which predicts little difference between the stabilization energies of the two dimer species in water.[25] The calculation suggests that the dimer−dimer interaction energy of the two side-on dimers fairly exceeds that of the two cyclic dimers.

Analysis of Low-Frequency Spectra. The presence of the isosbestic points at 210 cm^{-1} in the low-concentration region in Figure 6 may suggest the presence of the two states: the pure water cluster state and the acetic acid cluster state with the side-on type (and less probably cyclic) dimer unit(s). The latter state dominates the spectrum of the mixture with $x_A = 0.5$. As we saw in the case of ethanol/water mixtures,[1] the $R(\bar{\nu})$ spectra can be explained without the contribution from any pair of water and acetic acid, or could be as the sum of the $R(\bar{\nu})$ spectrum of pure water and that of the mixture with $x_A = 0.5$. Thus, the $R(\bar{\nu})$ spectra of binary solutions are decomposed into linear combinations of the $R(\bar{\nu})$ spectra of pure water and the mixture with $x_A = 0.5$:

$$R(\bar{\nu};x_A) = aR(\bar{\nu};x_A{=}0) + bR(\bar{\nu};x_A{=}0.5) \qquad (3)$$

where $R(\bar{\nu};x_A)$ is the $R(\bar{\nu})$ spectrum of an acetic acid/water binary solution with an acetic acid mole fraction of x_A, $R(\bar{\nu};x_A{=}0)$ is that of pure water, $R(\bar{\nu};x_A{=}0.5)$ is that of the 1:1 mixture, and a and b are the coefficients which should be calculated from the best-fit procedure. Decomposition of the $R(\bar{\nu};x_A)$ spectra was carried out with a conventional least-squares fitting method. The all $R(\bar{\nu};x_A)$ spectra were decomposed successfully into simple linear combinations, and Figure 9 shows some examples of the analysis for the spectra of the three mixtures with $x_A = 0.015$, 0.10, and 0.30. The coefficients a and b are plotted as a function of acetic acid mole fraction x_A in Figure 10. The fact that the mixture spectra are reproduced with linear combinations of the two basic spectra indicates that the mixtures are composed of the microscopic fragments of the two basic solutions. The dimer and small cluster units of water that characterize the low-

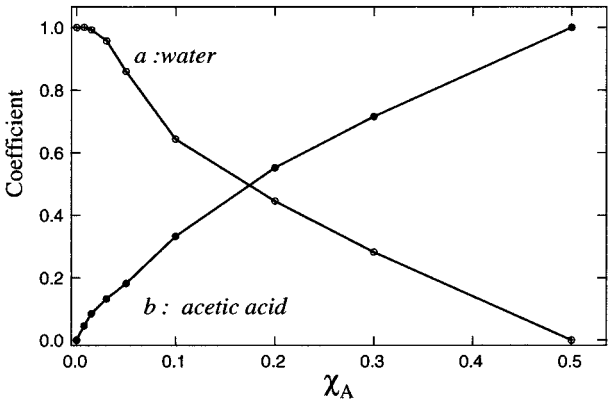

Figure 10. Concentration dependence of the coefficients of the water component (a) and the acetic acid cluster component (b) that are the $R(\bar{\nu})$ spectrum of the 1:1 mixture ($x_A = 0.5$).

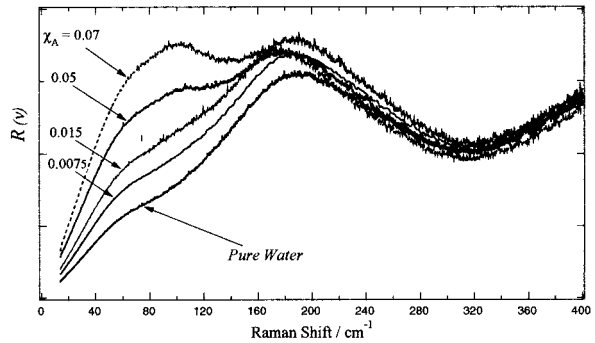

Figure 11. $R(\bar{\nu})$ spectra of aqueous solutions of acetic acid with $x_A = 0.0075$, 0.015, 0.05, and 0.07.

frequency spectra of water exist in the mixtures as fragments of liquid water, and such a unit in the 1:1 mixture must also exist in the intermediate region. This result is in accord with the microphase model of the aqueous mixtures proposed on the basis of ultrasonic absorption measurement.[3]

Hydrophobic Hydration. In the previous study, we measured the spectra with a mole fraction interval of 0.1 and observed the isosbestic point at 210 cm^{-1} in the low mole fraction region. Figure 11 shows the $R(\bar{\nu})$ spectra of the aqueous solutions with $x_A = 0.0075$, 0.015, 0.05, and 0.07. The $R(\bar{\nu})$ spectra in Figure 6 are for the solutions with $x_A \geq 0.10$. We can find intensity anomaly in the lower concentrations. The $R(\bar{\nu})$ spectra of the diluted solutions from $x_A = 0.05$ to 0.0075 exhibit surprising changes: (1) at $x_A = 0.0075$ the intensity of the water component increases more than that of pure water; (2) drastic intensity drop of the water component is seen at $x_A \geq 0.03$ (Figure 10). The intensity enhancement of the water component is synchronized with the drastic increase of the 1:1 mixture component. This means that the dimerization of acetic acid molecules becomes prominent at $x_A = 0.0075$. The anomaly (1) results in the deviation of the intensity from the isosbestic point at 210 cm^{-1}. One cannot see the isosbestic point in this lower concentration region. This is just because of the intensity enhancement of the water component around $x_A = 0.015$, as clearly seen in Figure 11. Figure 10 also indicates that the increase in the water component is accompanied by the intensity enhancement of acetic acid component at these low concentrations. Thus, we attribute the increase of the water component to "hydrophobic hydration" coupled with the generation of larger hydrophobic area due to the acetic acid clustering. This is what we saw in the mass spectrometric analysis of carboxylic acids in diluted aqueous solutions.[8] Apparently, this phenomenon is enhanced for the systems with larger alkyl chains. However,

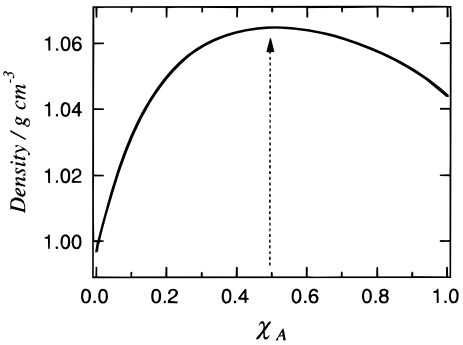

Figure 12. Density change of aqueous mixtures of acetic acid against mole fractions of acetic acid; data are taken from ref 26.

hydrophobic hydration requires numbers of water molecules sufficient for the construction of a hydrophobic shell covering the hydrophobic area. At concentrations higher than $x_A = 0.05$, the average number of water molecules for the shell formation around one solute molecule is smaller than 20 and any stable shell is not formed with the lower water numbers. This must be related to the result of the spectral change of the intramolecular OH stretching vibration of water molecules shown in Figure 5; the intensity of the O−H band of hydrogen bonded O−H group decreases eminently with increasing acid concentration at $x_A \geq 0.05$. Hydrophobic hydration can be seen at the diluted solute concentrations.

Three-State Model and Density Change. All the observed low-frequency spectra of the mixtures are reproduced simply by the linear combination of the pure water spectrum and that of the 1:1 mixture in the low-concentration region of $0 < x_A < 0.5$, and also by the combination of the spectrum of liquid acetic acid and that of the 1:1 mixture in the high concentration region, $0.5 < x_A < 1.0$. In addition to this fact, the observation of the two independent isosbestic points in the respective regions strongly suggests that there are three microscopic states of clusters (or aggregates): state 1, water cluster state in which intermolecular vibrations of water clusters are responsible for the low-frequency Raman spectrum of water; state 2, acetic acid cluster state with side-on type dimer units associated with dipole−dipole interaction, the Raman spectrum of the 1:1 mixture reflects the structure of this state; state 3, acetic acid cluster state with structures characteristic of liquid acetic acid. The densities of the mixtures[26] plotted as a function of acetic acid mole factions are shown in Figure 12. The density of the 1:1 mixture shows a maximum at $x_A = 0.5$ that indicates the presence of the closest packing of the molecules at this mixing ratio. The density change in Figure 12 clearly show the change of structures described by the three-state model.

Rayleigh Wing Spectra and Microphase Formation. Kaatze et al. presented a microphase model for carboxylic acid/water mixtures[3] and alcohol/water mixtures[4] on the basis of dielectric studies. Information on the presence of microphases composed of solute and/or solvent molecules can be also obtained from very low-frequency Raman spectra in the region $\bar{\nu} < 20$ cm^{-1}. Figure 13 shows Bose−Einstein (BE) corrected[27−29] very low-frequency Raman spectra of water (spectrum A), aqueous mixtures with $x_A = 0.0075$ (spectrum B) and 0.07 (spectrum C). As reported by Rousset et al.,[28] the water spectrum at 298 K exhibits a hump at 10 cm^{-1}. This signal is temperature dependent in intensity and position. The frequency increases with increasing temperature and falls to zero at −30 °C. Addition of a small amount of acetic acid in water enhances the wing intensity drastically, particularly in the region from 4 to 8 cm^{-1}.

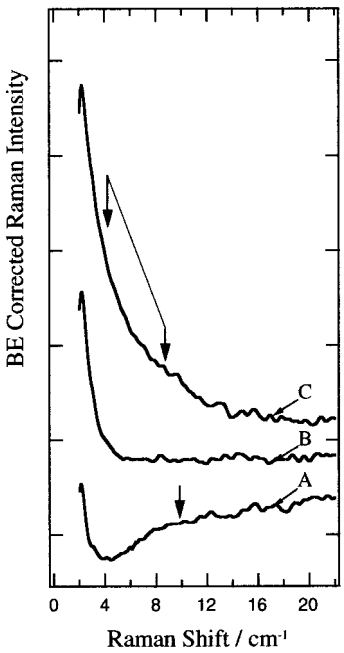

Figure 13. Bose−Einstein (BE) corrected very low frequency Raman spectra of water (A) and acetic acid aqueous solutions with $x_A = 0.0075$ (B) and 0.07 (C). Arrows indicate the peak positions or those of embedded components.

Interpretation of the low-frequency Raman component of water became very realistic after the simulation study by Madden and Impey.[10] They succeeded to explain the observed Raman band of water at 50 cm^{-1} with the motion of the molecular center of mass through the polarizability induced by dipole−dipole interaction between water molecules. Dipole−dipole interaction between the acetic acid clusters with large dipole moments is expected to induce strong Raman signals in the very low-frequency region. On the basis of the Raman studies of nuclei in glasses and silica particles in aerogels, Rousset et al. assumed that the low-frequency temperature-dependent Raman scattering comes from oscillations of transient water aggregates with a somewhat ordered structure. Ohmine[30] showed that the orientational relaxation coupled with long-range dipole−dipole interaction is responsible for the Raman spectrum of water at the low frequency of 5−20 cm^{-1}. The 10 cm^{-1} component in the water spectrum in Figure 13 must be related to this orientational relaxation of large water clusters. From this signal, Rousset et al. estimated the average size of the clusters at room temperature to be 11 Å. Because of longer sizes and larger dipole moments of the side-on type dimer and higher clusters with the dimer unit, orientational relaxation of the clusters is expected to take a much longer time than that of water. These factors may also result in the enhancement of the Raman intensity due to larger dipole−dipole interactions in the process of the orientational relaxation. The clusterization of acetic acid molecules with large dipole−dipole interaction thus provides us a reasonable elucidation for the enhanced activity of the very low frequency Raman component as compared with that of water. The microphase model is in accord with the present observation of the enhancement in the very low frequency component of the Raman spectra of the mixtures. As expected from the crystal structure of acetic acid, dipole−dipole interaction could be dominated in the acetic acid clusters elongating the lifetimes of the clusters in aqueous solutions.

On the basis of the measurement of excess partial molar enthalpies of small alcohols in aqueous solutions, Koga and co-workers reported the importance of solute−solute association in the concentrations as low as a solute mole fraction of 0.01.[31,32] In the mass spectrum of the ethanol/water mixture solution with an ethanol mole fraction of 0.01, we also observed dominant ethanol−ethanol association.[5] Generation of microphases in aqueous solution must be a general trend seen for most of the solute species, although their sizes may vary dependent on concentration, temperature, and particularly interaction energies. Islaelachvili presented some unifying concepts in intermolecular and interparticle forces.[33] On the basis of a theoretical consideration on a simple model, he showed that the associated state of like molecules is energetically preferred to the randomly dispersed state of a binary molecular mixture and there is always an effective attraction between like molecules. Water network formation is one of the strongest interactions in neutral molecular systems. Water−water association therefore induces solute−solute association in a binary mixture. In the case of acetic acid/water mixtures, acid−acid interaction itself also has a large energy and can generate a large dipole moment stabilized with an aqueous polar environment. Microphase formation in the binary mixtures is not so surprising in this sense. In Figure 14, we show a model structure of an acetic acid microphase on the basis of all the spectroscopic data shown in this report and the data by Kaatze et al.[3,4] The side-on dimer structure is an elementary unit in this model. Along the direction shown by an arrow, acetic acids stack up with alternating orientations of the methyl group to the carboxyl group. A very dense stacking of molecules can be seen for a structure with the side-on dimer unit. The model cluster is built up by considering the dipole−dipole interaction between acetic acid molecules and between the dimers, hydrophobic interaction between methyl groups, and electrostatic interaction (weak hydrogen bonding) between the carbonyl oxygen atom and the in-plane hydrogen atom of the methyl group. At this stage, this is just a model as a working hypothesis that must be subject to further critical theoretical and experimental examination.

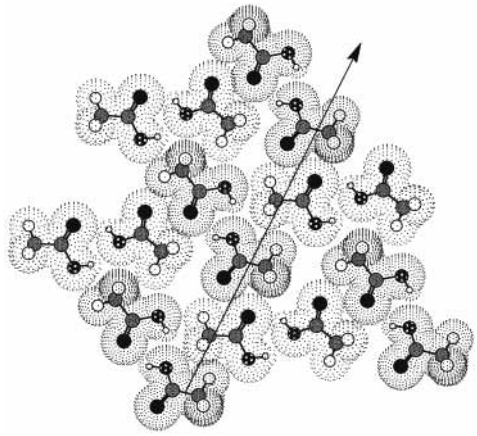

Figure 14. Model of an acetic acid microphase proposed based on the spectroscopic data.

References and Notes

(1) Egashira, K.; Nishi, N. *J. Phys. Chem. B* **1998**, *102*, 4054.
(2) Kosugi, K.; Nakabayashi, T.; Nishi, N. *Chem. Phys. Lett.* **1998**, *291*, 253.
(3) Kaatze, U.; Menzel, K.; Pottel, R. *J. Phys. Chem.* **1991**, *95*, 324.
(4) Brai, M.; Kaatze, U. *J. Phys. Chem.* **1992**, *96*, 8946.
(5) Nishi, N.; Takahashi, S.; Matsumoto, M.; Tanaka, A.; Muraya, K.; Takamuku, T.; Yamaguchi, T. *J. Phys. Chem.* **1995**, *99*, 462.
(6) Matsumoto, M.; Nishi, N.; Furusawa, T.; Saita, M.; Takamuku, T.; Yamagami, M.; Yamaguchi, T. *Bull. Chem. Soc. Jpn.* **1995**, *68*, 1775.
(7) Nishi, N.; Koga, K.; Ohshima, C.; Yamamoto, K.; Nagashima, U.; Nagami, K. *J. Am. Chem. Soc.* **1988**, *110*, 5246.
(8) Yamamoto, K.; Nishi, N. *J. Am. Chem. Soc.* **1990**, *112*, 549.

(9) Waldstein, P.; Blatz, L. A. *J. Phys. Chem.* **1967**, *71*, 2271.
(10) Madden, P. A.; Impey, R. W. *Chem. Phys. Lett*. **1986**, *123*, 502.
(11) Impey, R. W.; Madden, P. A.; McDonald, I. R. *Mol. Phys*. **1982**, *46*, 513.
(12) Sastry, S.; Stanley, H. E.; Sciortino, F. *J. Chem. Phys.* **1994**, *100*, 5361.
(13) Lund, P.-A.; Nielsen, O. F.; Praestgaard, E. *Chem. Phys. Lett*. **1978**, *28*, 167.
(14) Murphy, W. F.; Brooker, M. H.; Nielsen, O. F.; Praestgaard, E.; Bertie, J. E. *J. Raman Spectrosc.* **1989**, *20*, 695.
(15) Frisch, M. J.; Trucks, G. W.; Schlegel, H. B.; Gill, P. M. W.; Johnson, B. G.; Robb, M. A.; Cheeseman, J. R.; Keith, T.; Petersson, G. A.; Montgomery, J. A.; Raghavachari, K.; Al-Laham, M. A.; Zakrzewski, V. G.; Ortiz, J. V.; Foresman, J. B.; Cioslowski, J.; Stefanov, B. B.; Nanayakkara, A.; Challacombe, M.; Peng, C. Y.; Ayala, P. Y.; Chen, W.; Wong, M. W.; Andres, J. L.; Replogle, E. S.; Gomperts, R.; Martin, R. L.; Fox, D. J.; Binkley, J. S.; Defrees, D. J.; Baker, J.; Stewart, J. P.; Head-Gordon, M.; Gonzalez, C.; Pople, J. A. *GAUSSIAN 94*, revision C.3; Gaussian, Inc.: Pittsburgh, PA, 1995.
(16) Ng, J. B.; Shurvell, H. F. *J. Phys. Chem.* **1987**, *91*, 496.
(17) Ng, J. B.; Petelenz, B.; Shurvell, H. F. *Can. J. Chem.* **1988**, *66*, 1912.
(18) Bertie, J. E.; Michalian, K. H. *J. Chem. Phys*. **1982**, *77*, 5267.
(19) Nahringbauer, I. *Acta Chim. Scand*. **1970**, *24*, 453.
(20) Derissen, J. L. *J. Mol. Struct.* **1971**, *7*, 67.
(21) Herzberg, G. *Molecular Spectra and Molecular Structure II, Infrared and Raman Spectra of Polyatomic Molecules*; Krieger Publishing Co.: Malabar, FL, 1991; p 281.
(22) Hare, D. E.; Sorensen, C. M. *J. Chem. Phys*. **1992**, *96*, 13.
(23) Krishnamurthy, S.; Bansil, R.; Wiafe-Akenten, J. *J. Chem. Phys*. **1983**, *79*, 5863.
(24) Nakabayashi, T.; Kosugi, K.; Nishi, N., *J. Phys. Chem. A* **1999**, *103*, 8595.
(25) Nakabayashi, T.; Sato, H.; Hirata, F.; Nishi, N. Unpuiblished results.
(26) Washburn, E. W., Ed. *International Critical Tables, Vol. III*; McGraw-Hill: New York, 1928; pp 123−124.
(27) Walrafen, G. E. *J. Phys. Chem*. **1990**, *94*, 2237.
(28) Rousset, J. L.; Duval, E.; Boukenter, A. *J. Chem. Phys*. **1990**, *92*, 2150.
(29) Mizoguchi, K.; Hori, Y.; Tominaga, Y. *J. Chem. Phys*. **1992**, *97*, 1961.
(30) Ohmine, I. *J. Phys. Chem.* **1995**, *99*, 6767.
(31) Koga, Y.; Westh, P. *Bull. Chem. Soc. Jpn.* **1996**, *69*, 1505.
(32) Tanaka, S. H.; Yoshihara, H. I.; Ho, A. H.; Lau, F. W.; Westh, P.; Koga, Y. *Can. J. Chem*. **1996**, *74*, 713.
(33) Islaelachvili, J. N. *Intermolecular and Surface Forces*; Academic Press: Orlando, 1985; Chapter 9.